IEICE Electronics Express, Vol.16, No.8, 1–5

LETTER

Gain-clamped erbium-doped fiber amplifier using a Sagnac loop and low-reflectivity fiber Bragg grating

Kenichiro Tsuji[1a)] **and Tomoyuki Uehara**[1]

Abstract A gain-clamped erbium-doped fiber amplifier (GC-EDFA) can effectively suppress gain variations and optical surges that are often induced in the amplification of optical burst signals. In this paper, we demonstrate a simple and effective GC-EDFA using a Sagnac-loop-type EDFA with a low-reflectivity fiber Bragg grating (FBG). The gain-clamped characteristics and the experimental results of the dynamic response for an optical burst signal are presented.

Keywords: EDFA, gain clamp, optical burst signal, Sagnac loop, FBG
Classification: Optical hardware

1. Introduction

Erbium-doped fiber amplifiers (EDFAs) are widely used in optical fiber communication systems because of their excellent characteristics, including high efficiency, low noise, polarization insensitivity, and compatibility with optical fiber lines [1]. However, a conventional EDFA often causes significant gain variation when the input data stream has a long duration with no signal, such as a burst signal [2, 3, 4, 5, 6]. The gain variation often makes it difficult to decide the bit value in the receiver. In addition, shutdown of the input signal is unsuitable for conventional EDFAs because it sometimes causes optical surges when the input signal is recovered, which can damage the following devices in the optical system [7, 8, 9]. Thus, most practical EDFAs possess a safety interlock system which can automatically shut down the pump power dependent on the monitored input signal power, which complicates the whole EDFA system [10, 11].

An all-optical gain-clamped EDFA (GC-EDFA) is a solution for these problems [12]. In the GC-EDFA, a small signal gain is fixed to a predefined value by adding a partial optical feedback scheme that induces an internal oscillation when the input signal decreases under a threshold [13, 14, 15, 16, 17, 18]. The internal oscillation consumes the carrier density, and thus the signal gain is suppressed so that the gain is fixed regardless of the input signal power.

Most reported all-optical GC-EDFAs adopt an additional feedback fiber loop for the internal oscillation [19, 20, 21, 22, 23]. In this scheme, the output signal is often isolated using optical circulators so that the oscillation light does not appear at the output port [24]. The oscillation light propagates in the opposite direction with respect to the signal light in the gain medium (i.e., EDF) that enables wavelength adaptive amplification, and is not restricted by the oscillation wavelength. In contrast, Inoue proposed a novel wavelength adaptive configuration for a GC-EDFA using a Sagnac loop and a fiber Bragg grating (FBG) with a wavelength division multiplexing (WDM) coupler [25]. The advantages of this configuration are an intrinsic wavelength adaptive amplification owing to the loop property, and its simplicity, as it requires only one optical circulator. Excellent results of gain-clamped amplification at wavelengths close to the oscillation light have been shown, but detailed characteristics, such as noise performance and the wavelength dependence of the clamped gain variation, have not been presented.

In this paper, we present a modified version of the loop-type GC-EDFA in Ref. [25]. In our setup, the pump light is provided through a low-reflectivity FBG (LR-FBG) at the pump port. The configuration does not use a WDM coupler and hence is simpler, improving the cost effectiveness. We also show the detailed characteristics for our setup, including the noise characteristics and clamped-gain variations. The dynamic operation using pseudo optical burst signals is also experimentally demonstrated.

2. Configuration of the Sagnac-loop-based GC-EDFA

Fig. 1 shows a schematic diagram of our GC-EDFA based on a Sagnac loop. Pump and signal lights are injected from separate ports of the Sagnac loop interferometer, which includes an erbium-doped fiber (EDF) as a gain medium. The Sagnac loop includes polarization maintaining devices to guarantee full interference of the same polarization for the signal and oscillation light. An optical circulator in the signal port separates the input and output signals and produces an amplified signal at the output port. The 3-dB coupler of the Sagnac loop provides symmetrical bi-directional pumping without WDM couplers. In the loop-type EDFA, since the signal and pump ports are optically isolated due to the Sagnac effect, optical feedback for internal oscillation can readily be made between the Sagnac loop and the pump port provided that a partial reflector, such as an FBG, is inserted in the pump port. Thus, gain-clamped operation can be achieved by only adding an appropriately designed FBG to the loop-type EDFA. The

[1]Department of Communications Engineering, National Defense Academy, 1–10–20 Hashirimizu, Yokosuka-shi, Kanagawa 239–8686, Japan
a) kentsuji@nda.ac.jp

DOI: 10.1587/elex.16.20190056
Received January 24, 2019
Accepted March 1, 2019
Publicized March 22, 2019
Copyedited April 25, 2019

reflectivity of the FBG is a key parameter that determines the clamp gain of the GC-EDFA [27, 28]. The simplicity of the setup contributes to lower cost. The FBG does not affect the efficiency of pump power injection since the FBG is inherently low loss for pump wavelength. An optical isolator in the pump line may be required to protect the pump source since the internal oscillation emits toward the pump source.

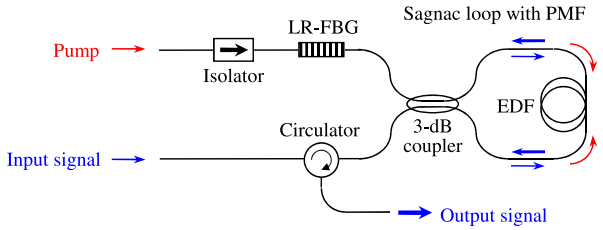

Fig. 1. Configuration of the Sagnac loop based GC-EDFA.

3. Experimental setup

We measured the gain-clamp characteristics of the loop-type GC-EDFA using the experimental setup shown in Fig. 2. The signal light from the wavelength switchable DFB-LD is modulated by a Mach–Zehnder type intensity modulator (MZ-IM) driven by an arbitrary function generator (AFG). The input signal power, which can be monitored with a power meter, is controlled by a variable optical attenuator (VOA), then input into the Sagnac loop EDFA. The output signal power is measured with an optical spectrum analyzer and the waveform is observed by a sampling oscilloscope with 20 GHz bandwidth via a photodiode (PD) with 50 GHz bandwidth. For the gain-clamped operation, an LR-FBG is inserted in the pump port. For comparison, we also use the same setup in Ref. [25] in which a high-reflectivity FBG with a VOA is connected through a WDM coupler (upper setup in Fig. 2). This conventional setup can control the effective reflectivity for internal oscillation by the VOA. Using the conventional setup, we investigated the appropriate reflectivity of LR-FBG for our simple setup that is a key parameter determining the clamp gain. As the result, we obtained an empirical formula as follows:

$$G_c = -3.78 \times \ln(R) + 19.1 \tag{1}$$

where G_c is clamp gain in dB and R is percent reflectivity of FBG with VOA. In the experiment, we use an LR-FBG of 2.0% reflectivity at 1530 nm with 0.3 nm bandwidth. From Eq. 1, 2.0% reflectivity can create sufficient clamp gain of about 16 dB for our measurement system and it is the lowest reflectivity considering the fabrication tolerances. As a pump source, we used a typical 1480-nm-band FP-LD and the power was set at 50 mW that is sufficient power for 16 dB gain. Although the pump power relates to the output saturation power, the clamp gain does not depend on the pump power because the excessive pump power is consumed by internal oscillation in the gain-clamped region.

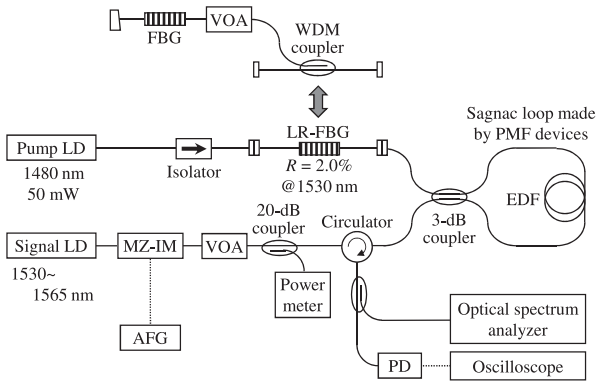

Fig. 2. Experimental setup.

4. Experimental results

First, we measured the gain characteristics using a continuous-wave signal at 1550 nm. Fig. 3 shows examples of the output optical spectra for input signal power P_{in}. We observed the internal oscillation spectrum at 1530 nm due to optical feedback by the LR-FBG in the pump port when the input signal power is under 150 µW.

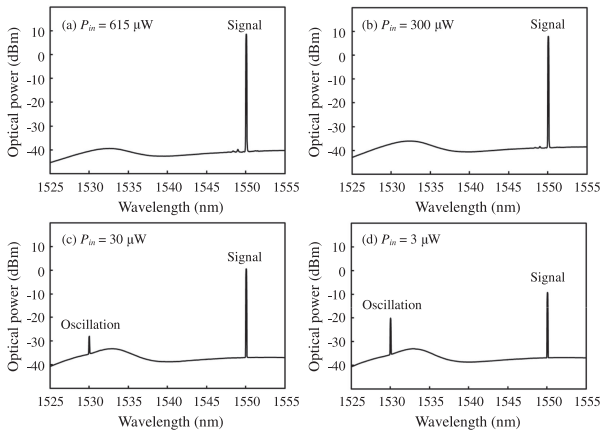

Fig. 3. Examples of output optical spectra when P_{in} is (a) 615 µW, (b) 300 µW, (c) 30 µW, and (d) 3 µW. Lower figures are the cases of gain-clamping.

These figures show that the internal oscillation can be occurred only when the input signal power is low. As a result, the output signal power is suppressed so that the gain is clamped during the internal oscillation. Note that the observed power of the oscillation light is leakage power from the imperfect Sagnac loop since these spectra are measured at the output port. We can estimate the noise figure from the measured output optical spectra using the following noise factor (NF) approximation [26]:

$$NF = \frac{1}{G} + \frac{P_{ASE}}{Ghv\Delta v} \tag{2}$$

where G is the signal gain, P_{ASE} is the amplified spontaneous emission (ASE) level at the signal wavelength, h is Planck's constant, v is the signal frequency, and Δv is the frequency resolution of the spectrum analyzer.

Figs. 4(a) and (b) show the measured signal gain and noise figure, respectively, as a function of input signal power when the signal wavelength is 1550 nm. The open black circles show the case without the LR-FBG (normal EDFA) and the solid red circles show the case with the LR-FBG in the pump port (GC-EDFA). The signal gain with the LR-FBG is practically constant for the small input power region, and we confirmed that internal oscillation occurs in that region. Although the noise figure increases slightly compared to the unclamped operation, the measured noise figure is less than 6 dB in the clamped-gain region. The values are equivalent to those for the conventional GC-EDFA with bi-directional pumping [19, 23]. These results confirm that our simple setup can be operated well as a GC-EDFA. The blue crosses show the conventional GC-EDFA as in Ref. [25] in which the LR-FBG is connected via a WDM coupler replacing the pair of FBG and VOA in upper setup of Fig. 2 by the LR-FBG. The gain and noise performance of our simple setup without a WDM coupler is almost equal to that with a WDM coupler [27, 28, 29]. Figs. 4(c) and (d) show the gain and noise figure as functions of the output signal power around the gain saturation region. The saturation output power of our setup was about 0.5 dB larger than that with a WDM coupler. We confirmed that the small increase of the saturation output power is due to the difference of insertion losses between LR-FBG and WDM coupler for pump wavelength (0.11 dB and 0.37 dB, respectively, in our setup). Although the insertion loss depends on the individual device, since the transmittance outside the reflection band of the FBG is inherently low-loss [30, 31, 32], our setup has good efficiency for pump injection comparable to the conventional setup with a WDM coupler.

Fig. 5 shows the dependence of the gain and noise figure on the signal wavelength in a GC-EDFA with an LR-FBG. The vertical axis indicates the averaged clamp gain for small input signal power from −45 to −25 dBm, in which the gain is well clamped to a constant value irrespective of signal wavelength. The wavelength dependence of the clamped gain is similar to the ASE spectrum in Fig. 3(c) and (d). In contrast, the noise figure is better for longer wavelengths, irrespective of the clamped gain. These characteristics are almost equivalent to a conventional GC-EDFA [26, 33]. This means that the wavelength dependence of the presented GC-EDFA is mainly governed by the original gain characteristics of the EDF.

5. Dynamic response to a burst signal

We also investigated the dynamic response using pseudo burst signals. Fig. 6 shows an example of the input burst signal at 100 Mbit/s, consisting of a 256-bit frame with a repetitive pattern of “0” and “1” with NRZ format and a time interval with no signal. We define the frame interval as $\Delta\tau$, as shown in the figure.

Fig. 7 shows the amplified burst signal at 1550 nm when the amplitude of input bit stream was about 120 μW and the $\Delta\tau$ was set to 6, 10, and 20 μs, respectively. The left column (a)–(c) shows the case of a loop-type EDFA without an LR-FBG, and the right column (d)–(f) shows the case of a loop-type GC-EDFA with an LR-FBG. In the case with an LR-FBG (GC-EDFA), the amplitude of the bit frame can be maintained to a constant value irrespective of $\Delta\tau$, whereas the amplitude without LR-FBG strongly depends on $\Delta\tau$. Since the average input signal power depends on $\Delta\tau$, the gain also depends on $\Delta\tau$ in

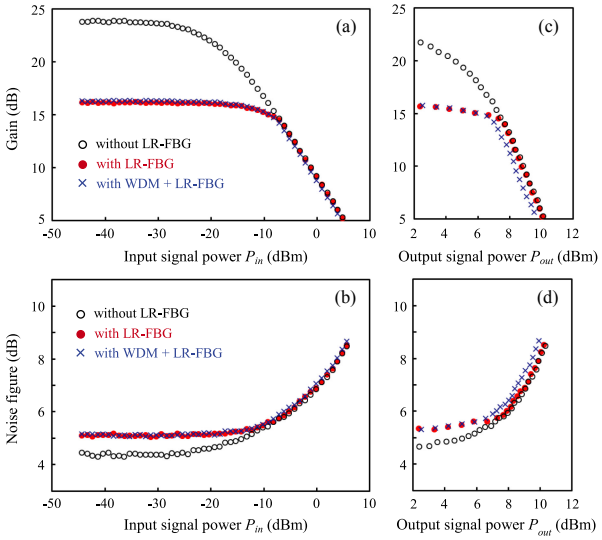

Fig. 4. Gain and Noise figure as a function of input/output signal power.

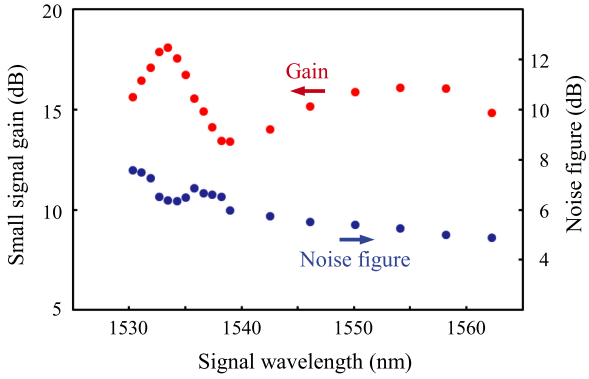

Fig. 5. Gain and noise figure dependence of the GC-EDFA with LR-FBG on the signal wavelength.

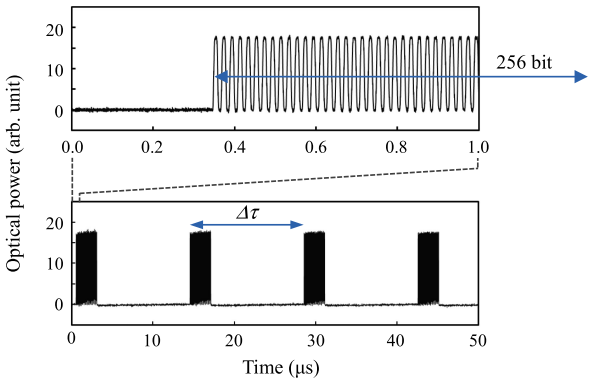

Fig. 6. Example of an input burst signal for the measurement of the dynamic response. The upper figure shows the waveform at the head of the bit frame.

normal EDFAs, and thus the amplitude of the bit frame varies according to $\Delta\tau$. In the GC-EDFA, since the gain is fixed to a constant value irrespective of the input power, the amplitude of the bit frame is also fixed to the value given by the reflectivity of the FBG.

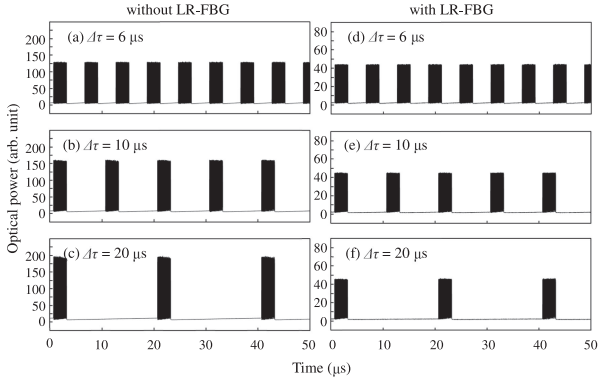

Fig. 7. Measured waveforms of the amplified signal for various frame intervals.

Fig. 8 shows the measured amplitude of the bit frame when $\Delta\tau$ was varied from 4 to 20 μs. The amplitude with an LR-FBG shows almost the same amplitude irrespective of $\Delta\tau$, whereas the one without an LR-FBG increases with $\Delta\tau$ and begin to saturate at about 20 μs. The amplitude variation for the presented GC-EDFA was less than 1.8%. Although there is an upper limit of input signal power for gain-clamped operation (about 60 μW in our setup), these results show that the presented simple setup can successfully operate as a GC-EDFA and could be useful for the amplification of burst signals.

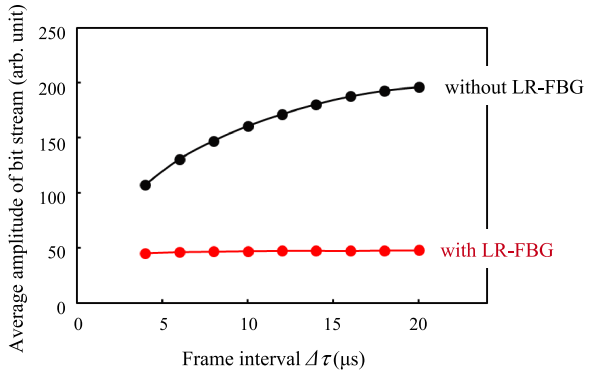

Fig. 8. Measured amplitude of bit frame as a function of frame interval $\Delta\tau$.

6. Conclusions

We experimentally demonstrated a loop-type GC-EDFA using a low-reflectivity FBG. The pump light is provided through an LR-FBG that contributes to cost effectiveness with comparable power efficiency to a conventional setup. Our simple setup without a WDM coupler showed a gain performance as good as configurations with a WDM coupler. We have also demonstrated a satisfactory dynamic response using a pseudo optical burst signal. Although the presented simple setup does not allow the clamped gain to be adjusted after installation, the gain adjustable function is not essential in practical applications. Because input dynamic range is managed in a process of system design and the clamp gain can be designed so as to match the system. In many applications, such as pre-amplifier for a receiver circuit, the requisite clamp gain can usually be predefined. The total gain can be modified with a VOA in the output port if it was needed after installation.

References

[1] P. Becker, *et al.*: *Erbium-Doped Fiber Amplifiers; Fundamentals and Technology* (Academic Press, New York, 1999) 1.
[2] A. V. Tran, *et al.*: "EDFA transient control based on envelope detection for optical burst switched networks," IEEE Photon. Technol. Lett. **17** (2005) 226 (DOI: 10.1109/LPT.2004.837736).
[3] B. J. Puttnam, *et al.*: "Experimental investigation of optically gain-clamped EDFAs in dynamic optical-burst-switched networks," J. Opt. Networking **7** (2008) 151 (DOI: 10.1364/JON.7.000151).
[4] H. H. Lee, *et al.*: "All-optical gain-clamped EDFA using external saturation signal for burst-mode upstream in TWDM-PONs," Opt. Express **22** (2014) 18186 (DOI: 10.1364/OE.22.018186).
[5] M. Karásek, *et al.*: "Gain stabilization in gain clamped EDFA cascades fed by WDM burst-mode packet traffic," J. Lightw. Technol. **18** (2000) 308 (DOI: 10.1109/50.827501).
[6] H. Feng, *et al.*: "Methods for stabilizing the gain of EDFAs in burst switching optical networks," Photonic Netw. Commun. **4** (2002) 151 (DOI: 10.1023/A:1015339328411).
[7] T. Tokura, *et al.*: "Quantitative analysis of optical surge propagation on transmission systems," IOOC-ECOC97 (1997) (DOI: 10.1049/cp:19971540).
[8] S. Furukawa, *et al.*: "Enhanced coherent OTDR for long span optical transmission lines containing optical fiber amplifiers," IEEE Photon. Technol. Lett. **7** (1995) 540 (DOI: 10.1109/68.384537).
[9] Y. Aoki, *et al.*: U.S. Patent 6064514 (2000).
[10] H. Ono, *et al.*: "An EDFA gain control and power monitoring scheme for fault detection in WDM networks by employing a power-stabilized control channel," J. Lightw. Technol. **20** (2002) 1335 (DOI: 10.1109/JLT.2002.800796).
[11] J. L. Shen, *et al.*: "L-band automatic-gain-controlled erbium-doped fiber amplifier utilizing C-band backward-amplified spontaneous emission and electrical feedback monitor," Appl. Opt. **48** (2009) 842 (DOI: 10.1364/AO.48.000842).
[12] M. Zirngibl: "Gain control in erbium-doped fiber amplifiers by an all-optical feedback loop," Electron. Lett. **27** (1991) 560 (DOI: 10.1049/el:19910353).
[13] S. W. Harun, *et al.*: "All-optical gain-clamped double-pass L-band EDFA based on partial reflection of ASE," IEICE Electron. Express **1** (2004) 171 (DOI: 10.1587/elex.1.171).
[14] J. T. Ahn, *et al.*: "Characterization of an ASE reflector-based gain-clamped Erbium-doped fiber amplifier," IEEE Photon. Technol. Lett. **17** (2005) 555 (DOI: 10.1109/LPT.2004.842380).
[15] S. W. Harun, *et al.*: "Gain clamping in L-band Erbium-doped fiber amplifier using a fiber Bragg grating," IEEE Photon. Technol. Lett. **14** (2002) 293 (DOI: 10.1109/68.986790).
[16] Y. Takushima and K. Kikuchi: "Gain spectrum equalization of all-optical gain-clamped Erbium-doped fiber amplifier," IEEE Photon. Technol. Lett. **11** (1999) 176 (DOI: 10.1109/68.740695).
[17] Q. Yu and C. Fan: "Simple dynamic model of all-optical gain-clamped Erbium-doped fiber amplifiers," J. Lightw. Technol. **17** (1999) 1166 (DOI: 10.1109/50.774249).
[18] S. W. Harun, *et al.*: "Gain clamping in two-stage L-band EDFA using a broadband FBG," IEEE Photon. Technol. Lett. **16** (2004) 422 (DOI: 10.1109/LPT.2003.822230).
[19] M. Cai, *et al.*: "Study on noise characteristic of gain-clamped Erbium-doped fiber-ring lasing amplifier," IEEE Photon. Technol. Lett. **9** (1997) 1093 (DOI: 10.1109/68.605511).

[20] J. T. Ahn and K. H. Kim: "All-optical gain-clamped Erbium-doped fiber amplifier with improved noise figure and freedom from relaxation oscillation," IEEE Photon. Technol. Lett. **16** (2004) 84 (DOI: 10.1109/LPT.2003.818906).
[21] A. A. A. Bakar, *et al.*: "Opto-optical gain-clamped L-band erbium-doped fiber amplifier with C-band control signal," Appl. Opt. **48** (2009) 2340 (DOI: 10.1364/AO.48.002340).
[22] K. Inoue: "Gain-clamped fiber amplifier with a short length of preamplification fiber," IEEE Photon. Technol. Lett. **11** (1999) 1108 (DOI: 10.1109/68.784203).
[23] C. H. Yeh, *et al.*: "S-band gain-clamped grating-based erbium-doped fiber amplifier by forward optical feedback technique," Opt. Express **14** (2006) 2611 (DOI: 10.1364/OE.14.002611).
[24] M. Kobayashi and S. Muro: "Gain stabilization in erbium-doped fiber amplifier with optical feedback loop using circulators," OECC'98 (1998) 98.
[25] K. Inoue: "Gain-clamped fiber amplifier with a loop mirror configuration," IEEE Photon. Technol. Lett. **11** (1999) 533 (DOI: 10.1109/68.759389).
[26] D. M. Baney, *et al.*: "Theory and measurement techniques for the noise figure of optical amplifiers," Opt. Fiber Technol. **6** (2000) 122 (DOI: 10.1006/ofte.2000.0327).
[27] T. Subramaniam, *et al.*: "All-optical gain-clamped Erbium-doped fiber-ring lasing amplifier with laser filtering technique," IEEE Photon. Technol. Lett. **13** (2001) 785 (DOI: 10.1109/68.935803).
[28] L. L. Yi, *et al.*: "Low noise figure all-optical gain-clamped parallel C+L band Erbium-doped fiber amplifier using an interleaver," Opt. Express **13** (2005) 4519 (DOI: 10.1364/OPEX.13.004519).
[29] L. Yi, *et al.*: "Tunable gain-clamped double-pass Erbium-doped fiber amplifier," Opt. Express **14** (2006) 570 (DOI: 10.1364/OPEX.14.000570).
[30] D. Grobnic, *et al.*: "Fiber Bragg gratings with suppressed cladding modes made in SMF-28 with a femtosecond IR laser and a phase mask," IEEE Photon. Technol. Lett. **16** (2004) 1864 (DOI: 10.1109/LPT.2004.831239).
[31] S. J. Mihailov, *et al.*: "Bragg gratings written in all-SiO_2 and Ge-doped core fibers with 800-nm femtosecond radiation and a phase mask," J. Lightw. Technol. **22** (2004) 94 (DOI: 10.1109/JLT.2003.822169).
[32] R. J. Williams, *et al.*: "Femtosecond direct-writing of low-loss fiber Bragg gratings using a continuous core-scanning technique," Opt. Lett. **38** (2013) 1918 (DOI: 10.1364/OL.38.001918).
[33] E. Desurvire: "Analysis of noise figure spectral distribution in erbium doped fiber amplifiers pumped near 980 and 1480 nm," Appl. Opt. **29** (1990) 3118 (DOI: 10.1364/AO.29.003118).